Kinetic Monte Carlo study of triplet-triplet annihilation in organic phosphorescent emitters

AIP | Journal of Applied Physics

Kinetic Monte Carlo study of triplet-triplet annihilation in organic phosphorescent emitters

H. van Eersel, P. A. Bobbert, and R. Coehoorn

Citation: Journal of Applied Physics **117**, 115502 (2015); doi: 10.1063/1.4914460
View online: http://dx.doi.org/10.1063/1.4914460
View Table of Contents: http://scitation.aip.org/content/aip/journal/jap/117/11?ver=pdfcov
Published by the AIP Publishing

JOURNAL OF APPLIED PHYSICS **117**, 115502 (2015)

Kinetic Monte Carlo study of triplet-triplet annihilation in organic phosphorescent emitters

H. van Eersel,[1,2] P. A. Bobbert,[1] and R. Coehoorn[2,1,a)]
[1]*Department of Applied Physics, Eindhoven University of Technology, P.O. Box 513, 5600 MB Eindhoven, The Netherlands*
[2]*Philips Research Laboratories, High Tech Campus 4, 5656 AE Eindhoven, The Netherlands*

(Received 21 November 2014; accepted 27 February 2015; published online 17 March 2015)

The triplet-triplet annihilation (TTA) rate in organic phosphorescent materials such as used in organic light-emitting diodes is determined predominantly either by the rate of single-step Förster-type triplet-triplet interactions, or by multi-step triplet diffusion. We show how kinetic Monte Carlo simulations may be used to analyze the role of both processes. Under steady state conditions, the effective triplet-triplet interaction rate coefficient, k_{TT}, which is often regarded as a constant, is found to depend actually on the number of excitons lost upon a triplet-triplet interaction process and to show a significant higher-order dependence on the triplet volume density. Under the conditions encountered in transient photoluminescence (PL) studies, k_{TT} is found to be effectively constant in the case of diffusion-dominated TTA. However, for the case of single-step TTA, a strongly different decay of the emission intensity is found, which also deviates from an analytic expression proposed in the literature. We discuss how the transient PL response may be used to make a distinction between both mechanisms. The simulations are applied to recently published work on the dye concentration dependence of the TTA rate in materials based on the archetypal green emitter tris[2-phenylpyridine]iridium ($Ir(ppy)_3$). © *2015 AIP Publishing LLC*.
[http://dx.doi.org/10.1063/1.4914460]

I. INTRODUCTION

At low current density and luminance levels, the internal quantum efficiency (IQE) of organic light-emitting diodes (OLEDs) containing Ir- or Pt-based phosphorescent emitters can reach values approaching 100%.[1–3] In these materials, the spin-orbit interaction induced by the heavy-metal atoms gives rise to exciton states with a quantum-mechanically mixed singlet and triplet character. Due to fast intersystem crossing (ISC), singlet states are almost instantaneously converted to triplet states, so that virtually all emission is due to phosphorescence. At high current densities, the IQE of phosphorescent OLEDs can show a strong roll-off.[4] One of the quenching mechanisms contributing to the roll-off is triplet-triplet annihilation (TTA). In the dilute host-guest emissive layer materials used commonly in phosphorescent OLEDs, TTA is viewed to be caused by a dipole-dipole (Förster-type) energy transfer process, again made possible by the admixture of a small amount of singlet character.[5,6] A TTA event may then be indicated schematically as $T_1 + T_1 \rightarrow S_0 + T_n \rightarrow S_0 + T_1$ or $T_1 + T_1 \rightarrow S_0 + T_n \rightarrow S_0 + S_0$, depending on how many excitons are lost. First, a triplet exciton is transferred to a molecular site at which a second triplet resides, leaving the first molecule in the ground state S_0. The second molecule is excited to a higher triplet state, T_n. Subsequently, the excited triplet relaxes non-radiatively to either T_1 or S_0, so that either one or both triplets are lost. The overall rate of the process is determined by the first step. We note that TTA processes can, in principle, also give rise to a singlet excited state (S_1).[7–9] However, for phosphorescent emitters, these states are almost immediately converted to triplets due to ISC, as mentioned above. Two extreme cases may be considered: (i) TTA occurs after exciton diffusion via intermediate dye molecules until the two excitons are at a distance less than a certain (small) capture radius ("multi-step"), or (ii) TTA occurs in between essentially immobile excitons as a result of a single long-range Förster-type dipole-dipole interaction process ("single-step").

The multi-step diffusion mechanism has been suggested first by Baldo *et al.*,[10] based on the observation from a transient photoluminescence (PL) study[11] that the TTA rate in dilute systems increases with increasing emitter concentration, as would be expected in the case of triplet percolation between nearby emitter molecules. Namdas *et al.*[12] and Ribiere *et al.*[13] adopted this point of view, and deduced from transient PL studies for a series of dendrimers with a tris(2-phenylpyridine)iridium ($Ir(ppy)_3$) core that the exciton hopping rate decreases exponentially with the hopping distance (R), consistent with an exchange (Dexter-type) interaction with a rate proportional to $\exp(-2R/\lambda)$. For the two sets of materials studied, including in Ref. 13 blends with a host material, the interaction decay length λ was found to be approximately 0.2 nm (Ref. 12) or 0.6 nm (Ref. 13). A similar analysis was recently presented by Zhang and Forrest,[14] who studied three archetypal phosphorescent organic light emitters based on Ir or Pt dye-complexes, including $Ir(ppy)_3$ in a $4,4'$–N,N'-dicarbazole-biphenyl (CBP) host. From a study of the concentration dependence in the 2–16 vol. % range, the authors argued that analyses in terms of the single-step mechanism would give rise to unrealistically large dipole-dipole interaction radii, and that Dexter-type triplet diffusion

a)reinder.coehoorn@philips.com

is rate-determining down to the smallest dye-concentration included. For the $Ir(ppy)_3$-based systems, the concentration dependence of the TTA rate was argued to be consistent with an interaction decay length $\lambda = 1.6$ nm. Interestingly, this value of λ is well outside the range of values deduced from experiment in Refs. 3 and 4, discussed above, as well as the 0.1–0.3 nm range obtained typically for the electron or hole wavefunction decay length from charge transport studies.[15–17]

In contrast, Staroske *et al*. have argued that at least for small emitter concentrations the single-step dipole-dipole mechanism is dominant.[18] In this study, and in subsequent work by Reineke *et al*.,[19] an effect of the concentration on the TTA rate observed in $Ir(ppy)_3$-based systems was regarded at least partially as of an extrinsic origin, resulting from fast diffusion on dye aggregates. We note that the studies of TTA in $Ir(ppy)_3$-based materials have been carried out for different matrix materials, including CBP,[10,13,14,20] $4,4',4''$-tris(*N*-carbazolyl)-triphenylamine (TCTA),[6,19] and a blend of bisphenol-*A*-polycarbonate and N,N'-diphenyl-N,N'-bis(3-methylphenyl)-(1, 1′-biphenyl)-4, 4′-diamine (PC and TPD),[21] and that the effect of the matrix due to, e.g., different degrees of triplet confinement on the guest and a different sensitivity to aggregation cannot be excluded.

In this paper, we first set out to make a step back, by investigating, using a kinetic Monte Carlo (MC) method, the validity of the underlying assumptions of the analyses used in the previous work. MC simulations have been applied earlier to study exciton diffusion and relaxation processes in organic materials[22–24] and excitonic processes determining the efficiency of photovoltaic devices.[25–27] We employ MC simulations to study how in a transient PL experiment the time-dependent emission varies as a function of both the dye and triplet exciton concentrations, for a range of realistic microscopic-scale parameters which describe the exciton diffusion and long-range dipole-dipole interaction processes. We consider a mixed mechanism in which both processes are included. As shown schematically in Fig. 1, the TTA rate is then at small dye concentrations determined predominantly by the rate of long-range dipole-dipole interactions, and it is enhanced by diffusion at large dye concentrations. In the presence of strong diffusion, when the multi-step mechanism is operative, the commonly used simplifying assumption that the TTA rate is proportional to the square of the triplet volume density, so that the effective triplet-triplet rate coefficient is independent of the triplet density, is found to be valid. However, in the absence of diffusion, i.e., in the single-step regime, we find that these assumptions do not hold anymore. We find that, as a consequence, the effective triplet-triplet rate coefficient which would follow from transient photoluminescence measurements can depend on the method of analyzing the data, and that the triplet-triplet rate coefficient which would follow from analyses of steady-state or transient experiments can be significantly different. The latter result is relevant when analyzing the efficiency loss processes leading to the roll-off of OLEDs under steady-state conditions. Furthermore, we find that then an often used analytical approach for TTA in a dilute host-guest system, within which the excitons are placed in an ordered manner on the points of a simple cubic grid with a site density equal to the exciton density (see, e.g., Refs. 12–14), is an oversimplification due to the neglect of the randomness of the exciton positions. We also show to what extent an expression for the time-dependence of the PL intensity in this regime, given in Ref. 18, should be corrected for an inconsistency already noted in Ref. 14.

The simulations thus show that, in general, the TTA rate cannot be described simply as a product of a *constant* triplet-triplet interaction coefficient times the square of the triplet volume density. Instead, a sufficiently complete description can only be given in terms of the microscopic scale parameters governing the exciton diffusion and dipole-dipole interaction rates. As a next step, we investigate the consequences of this finding for the analysis of transient PL studies of phosphorescent materials. We show from Monte Carlo

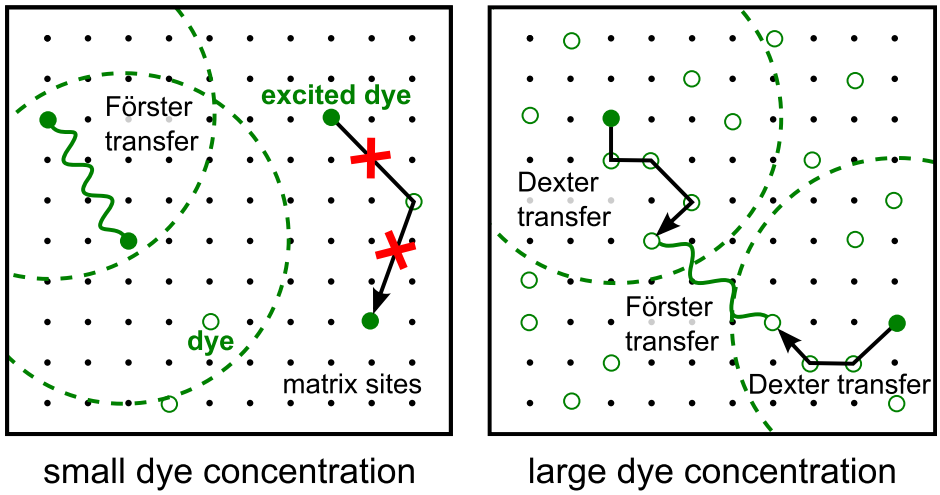

FIG. 1. Schematic diagrams indicating the relevant TTA mechanisms in matrix:emissive dye systems. TTA is described as resulting from a Förster-type interaction between two excitons (wavy curves). Multi-step Dexter-type exciton diffusion (black arrows) is a relatively short-range process, which can contribute to the TTA rate at large dye concentrations (right figure). At small dye concentrations (left figure), diffusion cannot contribute significantly (red crosses) due to the large distance between dyes, so that TTA is a single-step process. Matrix sites and excited (non-excited) dye-sites are indicated by small dots and closed (open) spheres, respectively. Dashed circles around the interacting excitons indicate which neighbor sites are at a distance smaller than the triplet-triplet Förster radius.

simulations that for devices such as studied in Ref. 14 the conventional method for analyzing the transient PL cannot be used to make a distinction between the single-step and multi-step processes, given the realistic experimental accuracy. In Ref. 14, the results of additional spectroscopic measurements were used to enable making such a distinction. As an alternative, we propose to exploit the dependence of effective triplet-triplet rate coefficient on the analysis method, mentioned above, for that purpose.

The paper is organized as follows. In Sec. II, we use MC simulations to analyze the TTA rate under steady-state conditions. In Sec. III, we focus on the time-dependence of the emission intensity as observed in transient PL experiments for a wide range of parameter values describing the single-step Förster-type and multi-step diffusion contributions. Based on these simulation results, the novel method for determining the predominant mechanism from the PL decay, mentioned above, is described. A comparison is given with the experimental results for $Ir(ppy)_3$-based materials studied in Ref. 14. Section IV contains a summary and conclusions. In the Appendix, a brief description is given of the kinetic MC simulation method used.

II. MONTE CARLO SIMULATION OF STEADY-STATE TRIPLET-TRIPLET ANNIHILATION

A. Simulation approach

Under steady-state conditions, the triplet rate equation describing the effects of radiative decay and bimolecular annihilation processes is given by

$$\frac{dT}{dt} = G - \frac{T}{\tau} - fk_{TT}T^2 = 0, \tag{1}$$

with T the triplet volume density, G the triplet generation rate, τ the triplet lifetime, f the annihilated fraction per triplet-triplet interaction event (1/2 or 1 if one or both triplets are annihilated), and k_{TT} the triplet-triplet interaction rate coefficient. Although not explicitly indicated, k_{TT} may depend on the triplet density. The triplet-triplet interaction of a first exciton with a second exciton at a distance R is described as a Förster transfer process with a rate

$$r_{F,TT}(R) = \frac{1}{\tau}\left(\frac{R_{F,TT}}{R}\right)^6, \tag{2}$$

where $R_{F,TT}$ is the Förster radius for this process. In order to deduce k_{TT} from Monte Carlo simulations, we study devices in which the molecular sites are points on a simple cubic lattice with an intermolecular distance $a_0 = 1$ nm. The layer thickness is 250 nm and the system lateral area is 25 000 nm^2; in the two lateral directions, periodic boundary conditions are applied. The simulations were carried out using the methodology presented in Ref. 28; more details are provided in the Appendix below. At the start of the simulations, a predetermined number of triplets[11] is present at random dye sites, corresponding to a triplet concentration c_T. The triplet volume density is thus $T = c_T a_0^{-3}$. The triplets can decay radiatively or they can be involved in a TTA process, upon which a loss of one or both triplets involved occurs (depending on the value of f). After such a process, one or two triplets are added at random dye sites, in order keep the triplet concentration fixed. From Eq. (1), the probability p_{TTA} that an exciton is lost due to TTA is given by

$$p_{TTA} = \frac{fk_{TT}T}{1/\tau + fk_{TT}T}, \tag{3}$$

which implies that

$$k_{TT}(T,f) = \frac{1}{f\tau T}\left(\frac{1}{p_{TTA}} - 1\right)^{-1}. \tag{4}$$

Statistically accurate values of the loss probabilities p_{TTA} were obtained by following the system during 50 to 100 times the radiative lifetime. We focus on the dynamic equilibrium situation, obtained after an initial equilibration period which typically ended after 10 times the radiative lifetime. In each case, several millions of radiative decay or TTA events were recorded.

B. No triplet diffusion

In this subsection, we study the TTA probability p_{TTA} in the absence of triplet diffusion. We consider systems for which the dye volume density is much larger than the triplet volume density, as in all systems studied experimentally. The TTA probability is then independent of the dye volume density. Figure 2 shows the triplet concentration dependence of the dimensionless quantity $k_{TT}\tau/a_0^3$, obtained for values of $R_{F,TT}$ equal to 3 and 5 nm, and for TTA upon which one (spheres) or both (triangles) triplets are lost. The triplet concentration range considered coincides with the range of starting concentrations employed in Ref. 14. The simulation for $R_{F,TT} = 3$ nm was included as this value was for $Ir(ppy)_3$ deduced theoretically from an analysis of the triplet emission and absorption spectra.[14] As the experimental results (shaded area in the figure) are indicative of value of $R_{F,TT}$ larger than 3 nm, also results for $R_{F,TT} = 5$ nm were included. It is generally assumed that the "one triplet lost" scenario is most relevant to phosphorescent host-guest materials used in OLEDs. The comparison with the "two triplets lost" scenario shows that at least part of the increase of k_{TT} with increasing triplet concentration is due to the effect of continuously adding excitons at random positions in order to maintain a constant exciton concentration. For the "two triplets lost" scenario, the resulting continuous short-distance triplet pair formation rate is larger than for the "one triplet lost" scenario, so that the annihilation rate is larger.

The dependence of k_{TT} on $R_{F,TT}$ may be understood by considering the emission efficiency from excitons surrounded by quencher molecules. In Ref. 29, this quencher method has been first applied to study the effect of TTA on the transient PL signal. The effective TTA rate coefficient as obtained from such an analysis is not expected to be necessarily the same as the coefficient obtained under steady state conditions. We will argue below that the application of the quencher method provides the rate coefficient, which would be expected within a "no excitons lost" scenario.

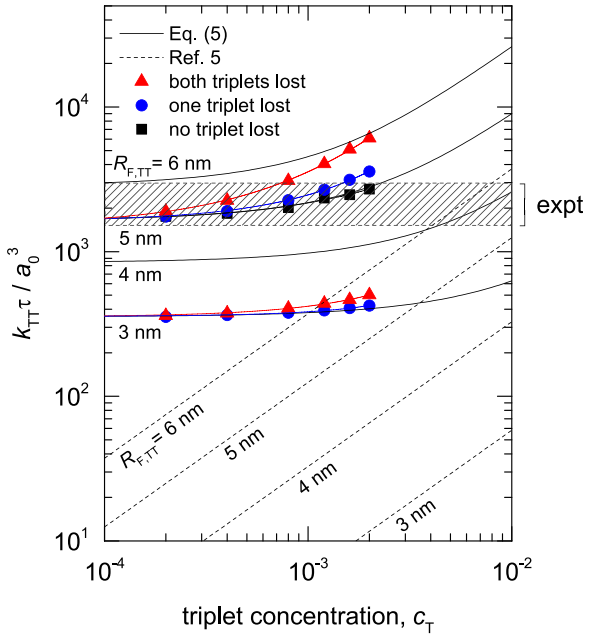

FIG. 2. Dimensionless steady-state triplet-triplet interaction rate coefficient in the absence of exciton diffusion, as a function of the triplet concentration and for various values of the $R_{F,TT}$. The solid and dashed curves give the analytical results obtained from Eq. (6) (this paper) and from Eqs. (4) and (5) in Ref. 14, respectively. The spheres and triangles give for $R_{F,TT} = 3$ and 5 nm the results of MC simulations with a loss of 1 or 2 triplets per interaction process, respectively. The squares give for $R_{F,TT} = 5$ nm the results of special MC simulations using the quenching probability of single excitons surrounded by quenching sites with a concentration $c_q = c_T$ (see text). The shaded region indicates the experimental range as observed from PL transients for a concentration $c_{T,0} \sim 0.002$ in Ref. 14.

The steady-state TTA rate may be deduced as follows. From the work of Förster,[5] the fraction of excitons which is lost due to Förster transfer to randomly distributed quenching sites with a volume density Q is given by

$$p_q = \frac{\pi}{2} C \exp\left(\frac{\pi}{4} C^2\right) \mathrm{erfc}\left(\frac{C\sqrt{\pi}}{2}\right), \tag{5}$$

with erfc the complementary error function and $C \equiv (4\pi/3) R_{F,TT}^3 Q \equiv V_F Q$. In analogy to Eq. (4), the quench rate coefficient k_q is then given by

$$k_q(Q) = \frac{1}{\tau Q}\left(\frac{1}{p_q(Q)} - 1\right)^{-1}. \tag{6}$$

The triplet-triplet interaction rate coefficient at a triplet volume density T is then equal to $2k_q$ ($Q = T$). The factor 2 arises in order to take into account that within the quenching process only unidirectional Förster transfer is included. It is of interest to express the final result, obtained by combining Eqs. (5) and (6), in the form of a series expansion

$$k_{TT}(T) = \pi \frac{V_F}{\tau}\left[1 + \left(\frac{\pi}{2} - 1\right) V_F T + O((V_F T)^2)\right]. \tag{7}$$

The zeroth-order term expresses that at small triplet concentrations the TTA probability p_{TTA} is of the order of the probability of finding an excited molecule within a volume V_F with radius $R_{F,TT}$. The higher-order terms are small as long as that probability is much smaller than 1. Apart from the factor of two, mentioned above, the zero-order term is well-known from the literature on the quench rate coefficient.[30]

As may be seen from Fig. 2, the analytical result (solid curves) is for small triplet concentrations in excellent agreement with the MC results. Just like the simulation results for the case of loss of one or two triplets, an increase of k_{TT} with the triplet concentration is expected from Eq. (7), albeit weaker than as found from the simulations within the "one exciton lost" or "both excitons lost" scenarios. This may be understood by noting that the quencher-method does not include a replacement of excitons, which have decayed radiatively or have been quenched, so that excitons which at the moment of their introduction in the system were quite isolated remain isolated. The analytical quencher-method results are consistent with the results of special MC simulations. In these special simulations, we calculate the quenching probability for single excitons added at random dye sites in a system containing a random distribution of quencher sites. Förster transfer to these quencher sites is immediate followed by non-radiative decay. This is shown in Fig. 2 for the case of $R_{F,TT} = 5$ nm (squares).

The zero-diffusion limit is expected to be most directly relevant to systems with a small dye concentration, so that long-range diffusion is severely hampered by a lack of percolation pathways. Although the values of k_{TT} as obtained for steady-state conditions can, in general, not be used to analyze result of transient PL experiments, as will be shown below, it is nevertheless of interest to make a preliminary comparison with experiment. In Fig. 2, the range of values of k_{TT} as deduced from transient experiments is shown (shaded region) for systems with a small (2 vol. %) concentration of the phosphorescent emitters Ir(ppy)$_3$) and bis(2-phenylpyridine)(acetylacetonate)iridium (Ir(ppy)$_2$(acac)) in a CBP host. The data were obtained in Ref. 14 from PL transients with at $t = 0$ a spot centre concentration around $c_{T,0} \sim 0.002$. If these systems are well below the percolation threshold, so that almost no exciton diffusion takes place, this comparison with steady-state simulation results would be indicative of Förster-radii around 5 nm. We discuss below the effects of exciton diffusion and of the transient nature of the experiment.

Figure 2 (dashed lines) also shows the triplet concentration dependence $k_{TT}\tau/a_0^3 \sim 8(R_{F,TT}/a_0)^6 c_T$ as deduced in Ref. 14 when neglecting the positional disorder of the triplets by positioning them on a simple cubic lattice. This is an oversimplification, as it may be seen that k_{TT} is then drastically underestimated. An analysis of transient PL data using this model, as was done in Ref. 14, would lead to a drastic overestimation of the Förster radii (up to ~11 nm).

C. Effect of exciton diffusion on the steady-state TTA rate

In this subsection, we describe TTA as a mixed process, in which the final TTA-inducing Förster triplet-triplet interaction step is preceded by multi-step triplet diffusion. Both Dexter and Förster mediated diffusion are included, with distance (R) dependent hop rates given by

$$r_{\mathrm{D,diff}}(R) = k_{\mathrm{D,0}} \exp\left(-\frac{2R}{\lambda}\right) \tag{8}$$

and

$$r_{\mathrm{F,diff}}(R) = \frac{1}{\tau}\left(\frac{R_{\mathrm{F,diff}}}{R}\right)^6, \tag{9}$$

respectively. Here, $k_{\mathrm{D,0}}$ is the Dexter hop rate in the zero-distance limit, λ is an effective interaction decay length related to the electron and hole wavefunction decay lengths, and $R_{\mathrm{F,diff}}$ is the Förster radius for triplet exciton diffusion. Just like Förster-mediated TTA, also Förster-mediated exciton diffusion is made possible by a small quantum-mechanical admixture of singlet character in the wavefunctions of the predominantly triplet-type excitons on the phosphorescent dye molecules used.

As an example, we analyze the role of diffusion for the case $R_{\mathrm{F,TT}} = 5$ nm. From the analysis given in the Subsection II B, this value is expected to provide an appropriate first estimate for the $Ir(ppy)_3$-based materials studied in Ref. 14. Figure 3 shows the $a \equiv c_{\mathrm{dye}}^{-1/3}$ dependence of k_{TT} at $c_{\mathrm{T}} = 0.002$ (solid curves) and 0.001 (dashed curves) for three values of $k_{\mathrm{D,0}}$, as obtained from steady-state MC simulations. A small Förster-type contribution to the triplet diffusion is included, characterized by a Förster radius equal to $R_{\mathrm{F,diff}} = 1.5$ nm, intermediate between typical experimental and theoretical values.[31] However, this is found to provide no significant contribution to the TTA rate. The simulations were carried out for a value $\lambda = 0.3$ nm, which is within the 0.2–0.6 nm range obtained from Refs. 12 and 13, and for a range of values of $k_{\mathrm{D,0}}$, which from a comparison with the experimental data for the $Ir(ppy)_3$-based systems (open spheres in Fig. 3) are expected to include a best-fit value. The simulations were carried out for 40 nm layers, as studied experimentally. This was found to introduce only a slight reduction of k_{TT}, around 5%, due to the reduced number of neighbor dye molecules near the surfaces. A triplet decay time $\tau = 1.0\,\mu$s is used, $a_0 = 1$ nm, and a loss of one triplet per TTA process is assumed. As a reference, the horizontal dashed line gives the value of k_{TT} in the zero-triplet density and zero-diffusion limit for an infinitely thick layer, obtained from Eq. (7).

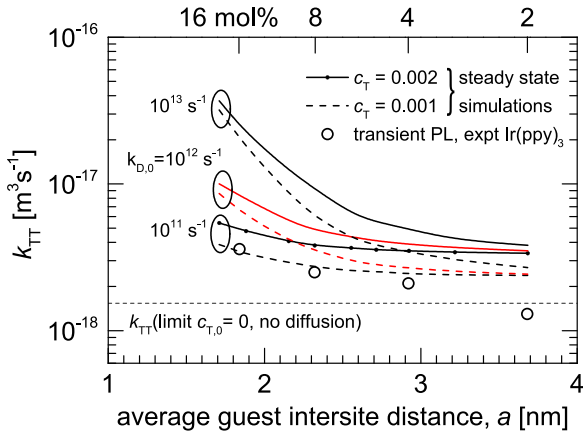

FIG. 3. Triplet-triplet interaction rate coefficient as a function of the average guest intersite distance (lower scale) or the dye concentration (upper scale) as obtained from MC simulations under steady-state conditions (solid and dashed curves), for the case $R_{\mathrm{F,TT}} = 5$ nm and for the triplet concentration and diffusion rate parameters given in the figure. For all cases, the data points were obtained for the dye concentrations indicated as small dots on one of the solid curves. The open circles give the experimental results for $Ir(ppy)_3$-based materials, obtained from transient PL experiments in Ref. 14.

The figure shows that at sufficiently small dye concentrations (large a), k_{TT} becomes independent of the dye concentration, and is determined only by the single-step process. A comparison between the simulated and experimental dye-concentration dependence in the 8%–16% range ($a = 1.8$–2.3 nm) would suggest a value of $k_{\mathrm{D,0}}$ around $1.0 \times 10^{11}\,\mathrm{s}^{-1}$, when making a comparison with the $c_{\mathrm{T}} = 0.002$ simulation results and when assuming $R_{\mathrm{F,TT}} = 5$ nm. However, as a result of the triplet concentration dependence of k_{TT}, it is necessary to explicitly consider the evolution of the quenching process during a transient PL experiment, as will be done in Sec. III.

III. MONTE CARLO SIMULATION OF PL TRANSIENTS

A. Simulation approach and analysis methods

In order to investigate to what extent transient PL studies probe the steady-state value of k_{TT}, we have carried out kinetic Monte Carlo simulations of the transient emission process. For that purpose, the time dependence of the emission is recorded after introducing at $t = 0$ triplets at random dye molecules in 40 nm thick layers, with a starting concentration $c_{\mathrm{T,0}} = 0.002$. A loss of one triplet per triplet-triplet interaction event was taken, the often-assumed value ($f = 1/2$). Typically, a lateral area of 400 000 nm^2 was considered (with periodic boundary conditions in the lateral directions), so that in each case the emission resulting from the generation of 32 000 excitons was studied. All simulations were done for $\tau = 1\,\mu$s and $a_0 = 1$ nm.

Figure 4(a) shows a typical result, obtained for a 16 mol. % layer with $R_{\mathrm{F,TT}} = 5$ nm, $\lambda = 0.3$ nm and $k_{\mathrm{D,0}} = 10^{12}\,\mathrm{s}^{-1}$. The simulations reveal a very fast initial drop of the emission rate: at the first data point shown (at 0.04 μs) it has already decreased by approximately 25% with respect to the value expected at $t = 0$ without TTA. A fair fit to the simulated PL intensity $I(t)$ beyond this short initial period can be made using the expression

$$\frac{I(t)}{I(0)} = \frac{2}{(2 + T_0 k_{\mathrm{TT}}\tau)\exp(t/\tau) - T_0 k_{\mathrm{TT}}\tau}, \tag{10}$$

with $T_0 = c_{\mathrm{T,0}} a_0^{-3}$ the initial triplet volume density. Equation (10) is the well-known solution of Eq. (1) for the case of a rate coefficient k_{TT}, which is independent of the triplet concentration and for $f = 1/2$. This expression, or a modified version which takes the effect of the T_0 variation across the optical spot into account, is conventionally used to analyze the experimental data (e.g., in Ref. 14). The value of k_{TT} could then be obtained from a least-squares fit to the measured log-$I(t)$ curve. However, such a fit is quite sensitive to the noise which is found in actual experiments as well as in simulations (see Fig. 4(a)), and also to the fast initial drop of the intensity, mentioned above.

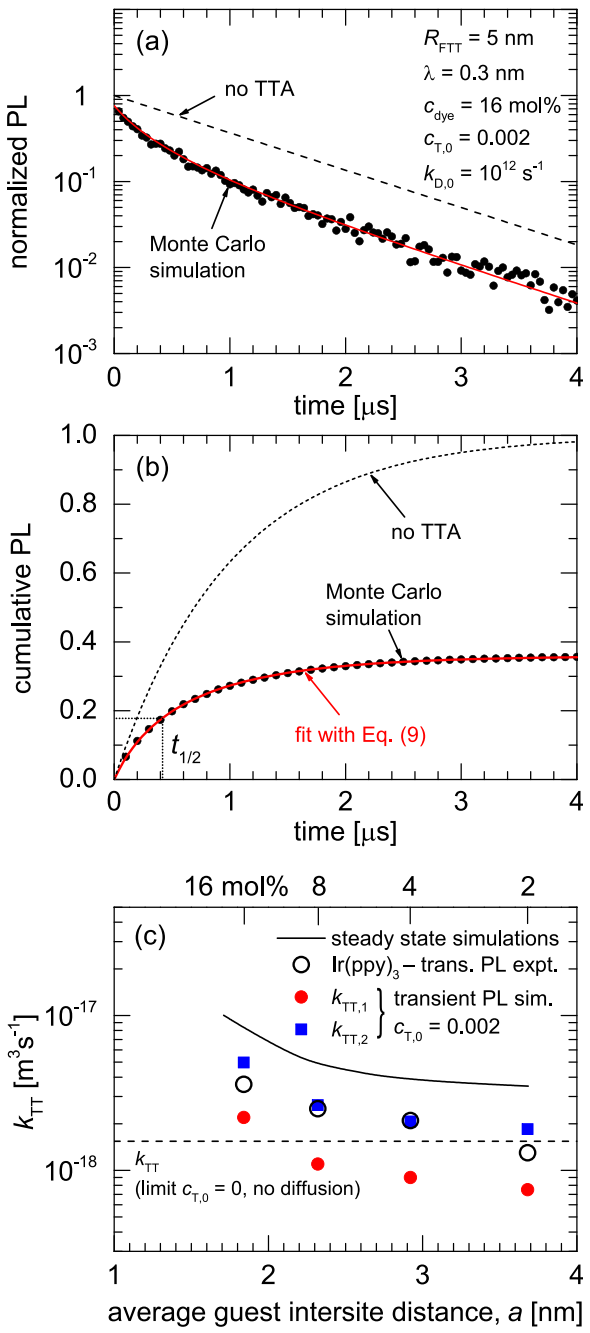

FIG. 4. Example of kinetic MC simulation results of a transient PL experiment, and of their analysis. (a) Time-dependent normalized PL intensity for the parameter values as indicated in the figure, and a fit based on Eq. (10) (solid red curve). The short-dashed line gives the PL intensity without TTA. (b) Normalized cumulative photoluminescence, for the case studied in figure (a) (black spheres), and a fit based on Eq. (10) (red curve). The resulting $t_{1/2}$ time is also indicated. (c) Triplet-triplet interaction rate coefficients $k_{TT,1}$ (solid red spheres) and $k_{TT,2}$ (solid blue squares) as deduced from the simulated transient PL intensity for systems as specified in figure (a), but with a variable dye concentration (and thus average guest intersite distance), for $c_{T,0} = 0.002$. For comparison, the values of k_{TT} as obtained under steady-state conditions at $c_T = 0.002$ (solid curve) and the experimental values as obtained in Ref. 14 for $Ir(ppy)_3$-based materials (open circles) are also included.

As a first alternative and more practical method, we therefore analyze the simulation data using the cumulative PL intensity, as shown in Fig. 4(b). We deduce a value $k_{TT,1}$ using Eq. (10) from the time $t_{1/2}$ at which half of the time-integrated emission has taken place (Fig. 4(b)). Note that this is *not* the time at which the intensity has decreased to 50% of the initial value. The red curve through the data points shown in Fig. 4(a) shows the emission decay as given by Eq. (10), with this rate coefficient and with the value of $I(0)$ taken as an adjustable parameter. This approach leads to a good fit of the simulation data. However, Eq. (10) then does not predict the fast decay observed in the first 40 ns time interval; the best fit value $I(0)$ is smaller than 1, viz., approximately 0.8.

The dye concentration dependence of $k_{TT,1}$ is shown in Fig. 4(c) (closed red spheres). For the 2 mol. % devices, no significant difference is found from simulations with $c_{T,0} = 0.001$ and 0.004 (not shown), but for larger dye concentrations a small dependence on the initial triplet density is found, up to approximately ±15% for the 16 mol. % devices. The relative change of $k_{TT,1}$ with the dye concentration is quite similar to that obtained under steady steady-state conditions, as may be seen from a comparison with the steady-state values obtained for $c_T = 0.002$ (solid curve in Fig. 4(c)). However, the absolute value of the quantity $k_{TT,1}$ deduced from a transient PL experiment is significantly smaller.

The example given above shows that Eq. (10) provides at best only an approximation. We ascribe this to a contribution of direct Förster-type transfer to the TTA rate. Engel *et al.*[29] have analyzed TTA due to direct Förster-type transfer, i.e., in the absence of diffusion. The authors proposed that the exact expression for the decay rate of the emission of excited randomly dispersed donors surrounded by randomly dispersed quenching sites, obtained by Förster,[5] may be used to deduce an effectively time-dependent value of k_{TT} in a transient PL experiment in which single-step Förster transfer determines the rate

$$k_{TT}(t) = \frac{2}{3}\pi R_{F,TT}^3 \sqrt{\frac{\pi}{\tau t}}, \tag{11}$$

and that from Eq. (1) the PL intensity then would be given by

$$\frac{I(t)}{I(0)} = \frac{\exp\left(-\frac{t}{\tau}\right)}{1 + \frac{2}{3}\pi^2 f T_0 R_{F,TT}^3 \mathrm{erf}\left(\sqrt{\frac{t}{\tau}}\right)}, \tag{12}$$

with erf the error function.[5] However, this result is at best a first approximation, because, as pointed out already by Zhang and Forrest,[14] in the derivation the time-dependence of the triplet density was not consistently included. We have investigated the accuracy of Eq. (12) by carrying out a series of MC simulations without diffusion. Periodic boundary conditions were employed. In all cases studied, the TTA rate is somewhat larger than expected from Eq. (12), so that the initial PL decay is somewhat faster. As an example, Fig. 5 shows the result for a system with $R_{F,TT} = 6$ nm, with an initial triplet concentration $c_{T,0} = 0.002$. The emission from 1 280 000 excitons was recorded. A convenient measure of the difference with Eq. (12) (solid red curve) is provided by the overall (time-integrated) PL efficiency, relative to the efficiency in the zero-T_0 limit,

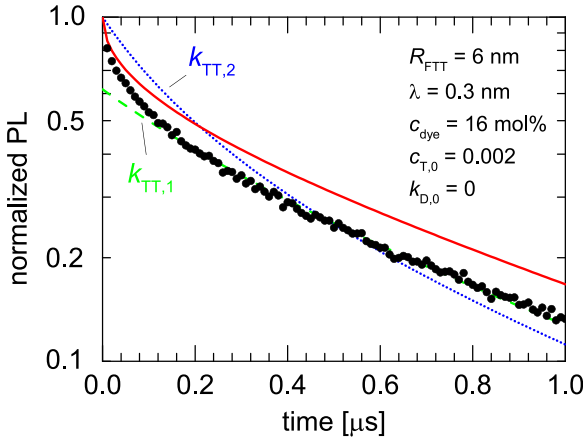

FIG. 5. Time-dependent PL intensity for a system without exciton diffusion, with $R_{F,TT} = 6$ nm. Closed spheres: result from MC simulations. Solid red curve: prediction from Eq. (12). Long green (short blue) dashed curves: fit to the simulated data using Eq. (10), with the rate coefficients $k_{TT,1} = 1.23 \times 10^{-18}$ s^{-1} and $k_{TT,2} = 3.62 \times 10^{-18}$ s^{-1}, respectively. The $k_{TT,1}$-curve has been renormalized (vertically shifted) such that a fair fit is obtained for a time larger than 0.1 μs.

$$\eta_{PL,rel}(T_0) \equiv \frac{\eta_{PL}(T_0)}{\eta_{PL}(0)}. \tag{13}$$

For the case studied, the MC simulation yields $\eta_{PL,rel} = 0.422$, whereas Eq. (12) yields $\eta_{PL,rel} = 0.515$. From Table I, which gives an overview of $\eta_{PL,rel}$ for other values of $R_{F,TT}$ and $c_{T,0}$, it may be seen that Eq. (12) indeed systematically underestimates the fraction of triplets lost due to TTA.

Although Eq. (10) was found to provide a fair description of the transient PL emission intensity (see Fig. 4(a)) for a case in which diffusion contributes significantly to the TTA rate, apart from a very short initial drop, it is in the single-step limit less accurate in a much wider time interval. This may be seen from Fig. 5, in which the long-dashed (green) curve shows a fit to the data using Eq. (10), with the rate coefficient $k_{TT,1}$ as obtained from the $t_{1/2}$ time and with a re-normalization such that the simulation data and the fit curve quite optimally coincide for a time larger than 0.1 μs. Within the $k_{TT,1}$-method, the short initial phase with a relatively large TTA rate obtains apparently a relatively low weight. It is therefore of interest to consider a second approach for deducing a value of k_{TT} from the transient PL data. For that purpose, we do not use the shape of the transient PL curve, as for $k_{TT,1}$, but the time-integrated relative PL intensity, defined by Eq. (13). For the case of a constant value of k_{TT}, it follows from Eq. (10) that

$$\eta_{PL,rel}(T_0) = -\frac{2\ln\left(\frac{2}{2 + T_0 k_{TT,2}\tau}\right)}{T_0 k_{TT,2}\tau}, \tag{14}$$

with $k_{TT,2} = k_{TT}$. We use this expression as an implicit definition of a second value of triplet-triplet interaction rate coefficient, $k_{TT,2}$. When k_{TT} is constant, $k_{TT,2} = k_{TT,1}$. However, when the effective value of k_{TT} decreases with time, $k_{TT,2}$ will be larger than $k_{TT,1}$, since more weight is given to the initial high-intensity part of the decay curve. Indeed, the ratio

$$r \equiv \frac{k_{TT,2}}{k_{TT,1}}, \tag{15}$$

as found from MC simulations without diffusion for $R_{F,TT} = 3$, 5, and 6 nm, is equal to 1.8, 2.4, and 2.9, respectively. Figure 4(c) (blue squares) shows that even when diffusion is included $k_{TT,2}$ can be significantly larger than $k_{TT,1}$ (red spheres). The values of $k_{TT,2}$ deduced using Eq. (14) from transient PL measurements are still somewhat smaller than the steady state values for a triplet concentration equal to the initial value in the PL experiment. For the example given in Fig. 5, neither the $k_{TT,1}$-method (green long-dashed curve) nor the $k_{TT,2}$-method (blue short-dashed curve) provides a satisfactory fit of the simulation data. However, we show in Subsection III B that it is useful to evaluate the ratio r as a means to make a distinction between the single-step and multi-step processes.

In the case of diffusion-dominated TTA, the triplet-triplet interaction rate coefficient depends on the diffusion coefficient, D. For an ordered simple cubic lattice, D is written as $D = a^2 r_{diff,tot}(a)/6$, with a the average nearest-neighbor distance between the dye molecules, and with $r_{diff,tot}(a)$ the effective *total* rate of exciton hops over that distance. In a transient PL experiment, k_{TT} is (from Ref. 29) given by

$$k_{TT}(t) = 8\pi D R_c \left(1 + \frac{R_c}{\sqrt{2\pi D t}}\right). \tag{16}$$

Here, R_c is an effective capture radius. The triplet-triplet interaction rate coefficient is thus effectively enhanced at short times. However, paradoxically, this is expected to be least relevant for the case of a large diffusion coefficient (in our case: large $k_{D,0}$ and c_{dye}) and a small capture radius (small $R_{F,TT}$). In Subsection III B, we show that indeed for sufficiently strong diffusion the ratio r becomes very close to 1.

TABLE I. Comparison of the relative PL efficiency $\eta_{PL,rel}$ as obtained from MC simulations without diffusion with the theoretical value as deduced from Eq. (12), for various Förster radii $R_{F,TT}$ and initial triplet concentrations $c_{T,0}$.

		$\eta_{PL,rel}$	
$R_{F,TT}$ [nm]	$c_{T,0}$	MC simulation	Eq. (12)
3	0.002	0.853 ± 0.004	0.890
5	0.001	0.718 ± 0.005	0.779
5	0.002	0.555 ± 0.003	0.643
5	0.004	0.383 ± 0.002	0.480
6	0.002	0.422 ± 0.002	0.515

B. Results, analysis, and discussion

In this subsection, we study the dependence of the transient PL response on the relevant interaction parameters, $R_{F,TT}$, $k_{D,0}$, and λ, and on the dye concentration. A comparison is given with the experimental results of Ref. 14 for Ir(ppy)$_3$-based systems, in order to investigate whether a conventional ($k_{TT,1}$) analysis could be used to separately deduce the three

interaction parameters, so that a distinction between the two mechanisms can be made. The dependence on the wavefunction decay length was studied by carrying out two sets of simulations, assuming Dexter diffusion with either $\lambda = 0.3$ nm or $\lambda = 1.6$ nm. The former value is typical for the hole and electron wavefunction decay length as found from charge transport studies,[15–17] and was employed in Sec. II C. The latter value was in Ref. 14 found to provide a good description of the experimental Ir(ppy)$_3$ data when assuming strong Dexter-type diffusion in combination with the value of $R_{F,TT}$ as deduced from spectroscopic experiments. Throughout this section, we give the dye-concentration dependence of k_{TT} in the form of plots of the quantity k_{TT}/a^2 as a function of the average intersite distance a. When the multi-step process is dominant, the diffusion coefficient is large, and the capture radius R_c may be viewed as a constant, it follows from the formalism discussed in Subsection III A that

$$\frac{k_{TT}}{a^2} = \frac{4\pi}{3} R_c r_{diff,tot}(a). \tag{17}$$

In the case of TTA dominated by Dexter processes, this ratio is thus expected to vary exponentially with a, with a decay length reflecting the distance dependence of the exciton hopping rate.[14]

We first discuss the simulations with $\lambda = 0.3$ nm. They were carried out with $R_{F,TT} = 3$, 5 and 6 nm, and with $k_{D,0} = 10^{11}$, 10^{12}, and 10^{13} s^{-1}, as also employed in Sec. II C. Under these conditions, the cross-over of TTA determined by single-step and multi-step processes can be studied. In Fig. 6, the ratio $k_{TT,1}/a^2$ is shown for all systems studied, with $k_{TT,1}$ an effective value obtained from the $t_{1/2}$ times (see Subsection III A). The short-dashed curve gives the value expected in the absence of diffusion, for an infinitely thick system, as obtained using Eq. (7). The long-dashed curve gives the diffusion-dominated value expected from Eq. (14) for the case $k_{D,0} = 10^{12}$ s^{-1}. We have assumed $R_c = R_{F,TT}$, as in our simulations the final capture process is due to a Förster-type triplet-triplet interaction, and write $r_{diff,tot}(a) = 6(r_{D,diff}(a) + r_{F,diff}(a))$ (using Eqs. (8) and (9), and noting that in a simple cubic lattice the total hop rate is six times the hop rate to one specific neighbor). The figure shows that at the largest dye concentration considered (16 mol. %, corresponding to $a = 1.84$ nm), k_{TT} is for all $R_{F,TT}$ values considered quite well predicted by the diffusion model. For $R_{F,TT} = 5$ and 6 nm and below approximately 6 mol. % ($a \geq 2.5$ nm), the single-step process is dominant. The intersection point of the short and long dashed thin curves yields a fair indication of the cross-over concentration between both regimes.

In Fig. 4, the open circles give the experimental data for the Ir(ppy)$_3$ systems studied in Ref. 14; the dashed heavy lines serve as a guide-to-the-eye. From a comparison with the simulation results, it may be concluded that it would be possible to explain the experimental data assuming a value of $R_{F,TT}$ slightly larger than 6 nm and the smallest value of the Dexter diffusion prefactor considered (10^{11} s^{-1}). In the absence of diffusion (short-dashed thin curves), or for diffusion with the largest Dexter prefactor considered, the

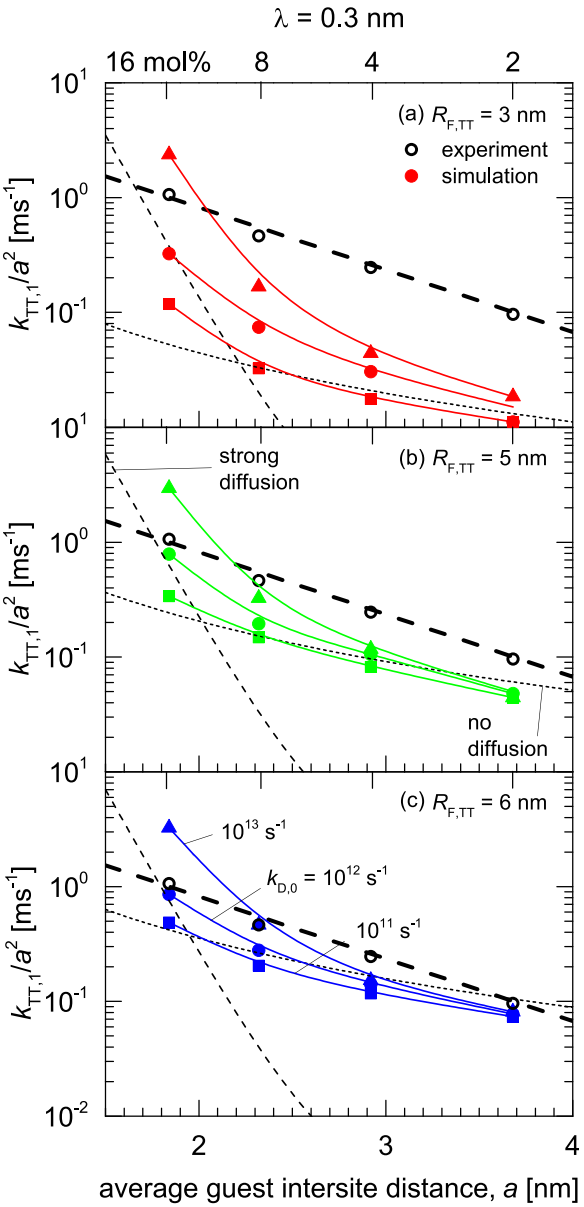

FIG. 6. The ratio $k_{TT,1}/a^2$ (symbols) as a function of the average guest intersite distance for $R_{F,TT}$ equal to (a) 3 nm, (b) 5 nm, and (c) 6 nm, obtained from MC simulations. The Dexter diffusion rate has been varied in a manner shown in figure (c), with an interaction decay length $\lambda = 0.3$ nm. The curves are guides-to-the-eye. The short dashed and long dashed thin curves give the theoretical values without diffusion and in the diffusion-dominated limit at $k_{D,0} = 10^{12}$ s^{-1}, respectively (see the text). The open circles, and the dashed heavy line which serves as a guide-to-the-eye, give the experimental values of k_{TT} as deduced in Ref. 14 for Ir(ppy)$_3$-based systems.

a-dependence as obtained from the simulations agrees less well with experiment. When assuming $\lambda = 0.3$ nm, it would then follow that for the two largest values of a considered (dye concentration 2 and 4 mol. %), the single-step mechanism is dominant, whereas for the smallest value of a considered (16 mol. %) the mechanism is more mixed. We remark that giving a detailed comparison with experiments is limited by their realistic experimental accuracy, related, e.g., to the accuracy of the starting triplet densities, the possible role of aggregation, and the possible role of concentration quenching. An indication of the possible role of such effects is the observation in Ref. 14 that for the largest dye concentration

considered, the triplet lifetime can be significantly smaller than for the smallest dye concentration.

A second set of simulations were carried out assuming $\lambda = 1.6$ nm, motivated above. Simulations were carried out with $R_{F,TT} = 1$ and 3 nm and a variable Dexter rate factor $k_{D,0}$, in order to explore cases in which the multi-step process dominates. Figure 7 shows the results for $R_{F,TT} = 3$ nm (close to the value $R_{F,TT} = 3.1$ nm obtained in Ref. 14 for the Ir(ppy)$_3$ systems) and $k_{D,0} = 10^8\,s^{-1}$. At a distance of 1.7 nm, the Dexter transfer rate is then equal to the transfer rate for the case $\lambda = 0.3$ nm with $k_{D,0} = 10^{12}\,s^{-1}$ discussed above. The ratio $k_{TT,1}/a^2$ varies to a good approximation linearly with a, as expected in this regime, although the slope of the line connecting the data points (not shown) is slightly larger than as expected from the theoretical value (Eq. (17), long dashed curve). We ascribe that to a somewhat diminished contribution of diffusion processes at small concentrations due to a lack of sufficient percolating pathways. If needed, further optimization of the fit quality would be straightforward; consistent with Eq. (17), k_{TT} is found to be proportional to $k_{D,0}$. The figure shows that using a value of λ close to 1.6 nm, and a small value of $R_{F,TT}$ in combination with an appropriately optimized value of the Dexter hop rate, good agreement with the experimental data (open circles) can be obtained.

The simulation results thus show that the three interaction parameters determining the TTA rate ($R_{F,TT}$, $k_{D,0}$ and λ) can, in general, not be deduced with sufficient accuracy from the results of transient PL experiments using the conventional ($k_{TT,1}$) method. We have therefore investigated whether the $k_{TT,2}$ method, which employs the time-integrated PL efficiency, could be used to enrich the experimental data, viz., by using the $k_{TT,2}/k_{TT,1}$-ratio r. Figure 8 shows r as a function of the average intersite distance when $\lambda = 0.3$ nm and $R_{F,TT} = 3$, 5, and 6 nm (set I, red, green, and blue data points and curves, respectively), with $k_{D,0} = 10^{-12}$ s^{-1}. The ratio r increases

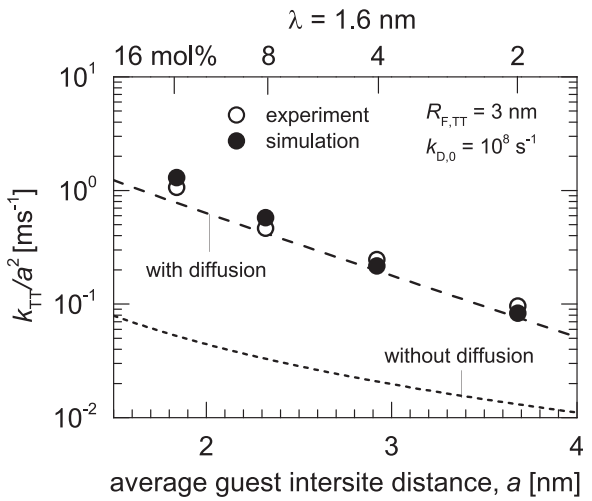

FIG. 7. The ratio $k_{TT,1}/a^2$ (closed spheres) as a function of the average guest intersite distance, obtained from MC simulations, assuming Dexter diffusion with an interaction decay length $\lambda = 1.6$ nm. The other simulation parameters are as given in the figure. As in Fig. 6, the short dashed and long dashed curves give the theoretical values without diffusion and in the diffusion-dominated limit, respectively, and the open circles give the experimental values of k_{TT} as deduced in Ref. 14 for Ir(ppy)$_3$-based systems.

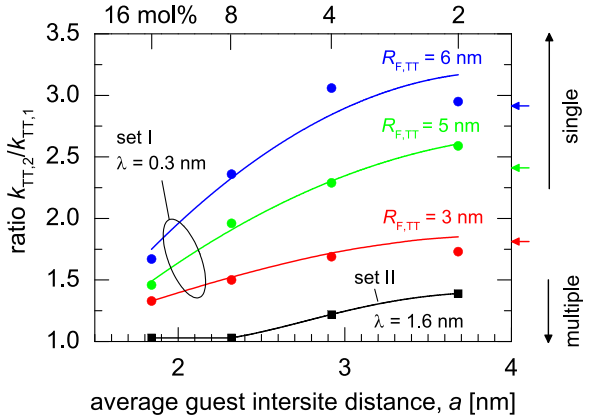

FIG. 8. The rate coefficient ratio r for set I ($\lambda = 0.3$ nm) and set II ($\lambda = 1.6$ nm), the two sets of simulations discussed in Sec. III B, for $k_{D,0} = 10^{12}\,s^{-1}$. The solid curves are guides-to-the-eye. The simulation results obtained in the absence of diffusion are indicated by the horizontal arrows at the right axis. The single-step and multi-step regimes are indicated by the vertical arrows, with a cross-over around $r \sim 2$.

when due to an increasing value of $R_{F,TT}$ or due to an increasing average intersite distance the single-step process becomes more predominant. We find that in the single-step (multi-step) regime, r is well above (below) a cross-over value of approximately 2. The cross-over dye concentration is defined as the value at which diffusion enhances k_{TT} by a factor of 2 with respect to the single-step value. The curves are a guide-to-the-eye. The numerical accuracy of the data points, $\pm(0.1–0.2)$, is determined almost completely by the accuracy of $k_{TT,1}$. For the 2 mol. % systems, r approaches the zero-diffusion values given in Subsection III A (arrows in the figure). The black data points and curve in Fig. 8 give the r ratio for the systems with $\lambda = 1.6$ nm, studied in Fig. 7 (set II). For large dye concentrations, the predominant role of diffusion leads to values of the ratio $r \equiv k_{TT,2}/k_{TT,1}$ close to 1. Only at small dye concentrations, a small role of single-step TTA is visible. This finding further confirms that measuring the ratio r would provide a simple method for directly determining which contribution to the TTA process dominates.

It follows from the analysis given above that the conventional ($k_{TT,1}$) method for analyzing the transient PL decay process will often provide insufficiently rich information to separately determine the most relevant interaction parameters $R_{F,TT}$, $k_{D,0}$, and λ. In particular, it follows that an approximately linear variation of the ratio k_{TT}/a^2 with a does not necessarily imply that the TTA process is in the diffusion-controlled regime over the entire dye-concentration range studied. For the case of the Ir(ppy)$_3$ systems studied in Ref. 14, for example, we have found that the experimental data could be explained with a relatively large value of $R_{F,TT}$, slightly larger than 6 nm, and weak diffusion (a relatively small interaction decay length of $\lambda = 0.3$ nm and a relatively small Dexter prefactor), as well as using a relatively small value of $R_{F,TT}$ in combination with strong diffusion (a large interaction decay length of $\lambda = 1.6$ nm). The simulation results reveal that an independent spectroscopic measurement of $R_{F,TT}$ could be used to determine the two other interaction parameters with good accuracy. The value $R_{F,TT} = 3.1$ nm obtained in Ref. 14 for the Ir(ppy)$_3$ systems,

e.g., indeed implies that for these systems λ is approximately 1.6 nm, as stated in Ref. 14, so that the diffusion mechanism is predominant. We note that such a λ-value is unexpectedly large. Studies of Dexter energy exchange reveal a wide range of interaction decay lengths, ranging from less than 0.1 nm for through-space coupling to more than 2 nm. However, such a large interaction distance is only obtained for coupling through covalently connected bridging units.[32] In order to better understand the possible large value of λ for the case of $Ir(ppy)_3$ molecules embedded in a matrix material, it would be of interest to investigate in more depth the long-range Dexter coupling as mediated by the triplet states of the matrix molecules, acting as virtual intermediate levels. Application of the k_{TT}-ratio method would be an alternative method for obtaining independent information about the interaction parameters. Two simple transient PL measurements, one at a fluence well in the TTA regime and one in the limit of zero fluence, will suffice. The ratio r can then be obtained from the ratio of $k_{TT,1}$ as determined by fitting the transient data with Eq. (10) and $k_{TT,2}$ as determined by Eq. (14), using the PL efficiency normalized by the PL efficiency in the limit of zero fluence. Advantageously, the method can already be used when only a single sample is available, so that no dye concentration-dependent measurements are necessary.

IV. SUMMARY AND CONCLUSIONS

Kinetic Monte Carlo simulations under steady-state and transient conditions have been used to study the relative contributions of single-step Förster-type transfer and multi-step Dexter-type diffusion to the TTA rate in phosphorescent emitter materials as used in OLEDs. From the steady-state simulations, we have found the following. (i) The triplet-triplet interaction rate coefficient k_{TT} is constant at small triplet concentrations, c_T, but shows a significant higher-order dependence on c_T at high triplet concentrations. The results are at variance with the predictions obtained within the often-used ordered lattice approximation, which yields a linear dependence of k_{TT} on c_T. (ii) The rate coefficient k_{TT} depends in a non-trivial way on the number of triplets lost upon a triplet-triplet interaction event.

The transient PL simulations used to study TTA under non-steady state conditions reveal that: (i) the time-dependent PL intensity cannot be described assuming a constant value of k_{TT}, (ii) from a comparison of two different values of k_{TT}, deduced from the measurements using two different methods, a distinction can be made between TTA predominantly due to single-step or multi-step processes, and (iii) these transient values of k_{TT} are significantly smaller than the steady-state value obtained for the triplet concentration at time $t = 0$.

A comparison of the simulation results with experimental results for $Ir(ppy)_3$-based materials shows that the data are consistent with the multi-step scenario put forward in Ref. 14. Good agreement with the experimental data was found when using a radius for Förster-type triplet-triplet interactions equal to $R_{F,TT} = 3$ nm, close to the value deduced from spectroscopic experiments in Ref. 14, and when using an exciton wavefunction decay length $\lambda = 1.6$ nm, close to the value suggested in Ref. 14. We find that using the measured value of $R_{F,TT}$ as a constraint was important. When leaving $R_{F,TT}$ as a free parameter, the simulations show that also a smaller value of λ, down to approximately 0.3 nm, in combination with a larger value of $R_{F,TT}$, up to approximately 6 nm, would be consistent with the experimental data given in Ref. 14. At small dye concentrations, below approximately 5 mol. %, TTA would then predominantly be due to single-step Förster transfer, as suggested by Staroske and co-workers.[18] This shows that additional information is required to unambiguously determine the TTA mechanism. As an alternative method for obtaining such additional information, we have proposed to determine the $k_{TT,2}/k_{TT,1}$ ratio defined in Eq. (15). Advantageously, this also makes it possible to determine already for one selected dye concentration which contribution is most important.

In dilute organic phosphorescent emitter materials, exciton diffusion not only influences the TTA rate but also the rate of other excitonic interaction processes. Examples are the energy transfer to a lower energy acceptor, quenching at polarons or extrinsic defects, and concentration quenching.[31,33] It would be of interest to use Monte Carlo studies as well to investigate to what extent in relevant materials systems these interactions are single-step or multi-step, and to what extent a quantitatively consistent description of the diffusion rate is obtained. Such simulations should also include various refinements, such as the effect of exciton energetic disorder on the diffusion process (see, e.g., Ref. 34 and references therein) and the possible occurrence of emitter aggregation.[3,19]

ACKNOWLEDGMENTS

We thank Professor Janssen, Professor Adachi, Dr. Goushi, and Dr. Yonehara for stimulating comments and Dr. Veldman for useful remarks. This work was supported by the Dutch nanotechnology program NanoNextNL (HvE).

APPENDIX: MONTE CARLO SIMULATION METHOD

In this Appendix, we give a short overview of the steps involved in the kinetic Monte Carlo simulations. The system sizes used in order to obtain results with a sufficient precision are discussed in the main text. At the start of the simulations, the system to be studied is initialized in a manner described already in detail in Sec. II A of the main text: triplets are placed at random dye sites, corresponding to a certain starting triplet concentration. Subsequently, the following steps are used for obtaining the TTA rate coefficient under steady-state or transient conditions. The methodology is similar to that used by Bässler when studying hopping transport in disordered organic semiconductors.[15]

Step 1. Calculation of the rate for each possible event: For each exciton, the rates for the transfer to each neighbor up to a certain cut-off radius are calculated. The possible events included are the transfer to another exciton (leading to a TTA process), with a rate given by Eq. (2), and the transfer to empty sites (leading to exciton diffusion) due to a

Dexter process, with a rate given by Eq. (8), or due to a Förster process, with a rate given by Eq. (9). For each possible event i, the rate r_i is then available. The total number of events is N.

Step 2. Event selection: The next event which will take place is selected in the following way. First, for each event i the partial sum $S_i \equiv \sum_{k=1}^{i} r_k$ is calculated. Subsequently, a random number u is drawn from the interval $(0, r_T]$, with $r_T = \sum_{k=1}^{N} r_k$ the total of all rates. From all possible events, the event i for which $S_{i-1} < u \leq S_i$ holds is selected.

Step 3. Event execution: The positions of the excitons on the lattice are updated according to the event selected. In the case of TTA, one or both of the excitons involved are lost. For steady-state simulations, one or two excitons, respectively, are then added on random unoccupied guest sites, in order to keep the exciton concentration constant.

Step 4. Simulation time update: The time passed for this event is drawn from an exponential distribution with an expectation value equal to $1/r_T$.

For steady-state simulations, these steps are iterated until a stable dynamic equilibrium situation has been obtained and a sufficient accuracy level has been reached (see also the last paragraph of Sec. II A). For transient simulations, these steps are iterated until all excitons have been lost due to radiative decay or TTA.

[1]C. Adachi, M. A. Baldo, M. E. Thompson, and S. R. Forrest, J. Appl. Phys. **90**, 5048 (2001).
[2]M. C. Gather, A. Köhnen, and K. Meerholz, Adv. Mater. **23**, 233 (2011).
[3]Q. Wang, I. W. H. Oswald, X. Yang, G. Zhou, H. Jia, Q. Qiao, Y. Chen, J. Hoshikawa-Halbert, and B. E. Gnade, Adv. Mater. **26**, 8107 (2014).
[4]C. Murawski, K. Leo, and M. C. Gather, Adv. Mater. **25**, 6801 (2013).
[5]T. Förster, Z. Naturforschung A **4**, 321 (1949).
[6]S. Reineke, K. Walzer, and K. Leo, Phys. Rev. B **75**, 125328 (2007).
[7]D. Y. Kondakov, J. Soc. Inf. Disp. **17**, 137 (2009).
[8]D. Y. Kondakov, T. D. Pawlik, T. K. Hatwar, and J. P. Spindler, J. Appl. Phys. **106**, 124510 (2009).
[9]H. Fukagawa, T. Shimizu, N. Ohbe, S. Tokito, K. Tokumaru, and H. Fujikake, Org. Electron. **13**, 1197 (2012).
[10]M. A. Baldo, C. Adachi, and S. R. Forrest, Phys. Rev. B **62**, 10967 (2000).
[11]We note that in PL studies of these materials essentially all singlet excitons made are almost instantaneously converted to triplets by ISC.
[12]E. B. Namdas, A. Ruseckas, I. D. W. Samuel, S.-C. Lo, and P. L. Burn, Appl. Phys. Lett. **86**, 091104 (2005).
[13]J. C. Ribierre, A. Ruseckas, K. Knights, S. V. Staton, N. Cumpstey, P. L. Burn, and I. D. W. Samuel, Phys. Rev. Lett. **100**, 017402 (2008).
[14]Y. Zhang and S. R. Forrest, Chem. Phys. Lett. **590**, 106 (2013).
[15]H. Bässler, Phys. Status Solidi B **175**, 15 (1993).
[16]O. Rubel, S. D. Baranovskii, P. Thomas, and S. Yamasaki, Phys. Rev. B **69**, 014206 (2004).
[17]B. Baumeier, O. Stenzel, C. Poelking, D. Andrienko, and V. Schmidt, Phys. Rev. B **86**, 184202 (2012).
[18]W. Staroske, M. Pfeiffer, K. Leo, and M. Hoffmann, Phys. Rev. Lett. **98**, 197402 (2007).
[19]S. Reineke, G. Schwartz, K. Walzer, M. Falke, and K. Leo, Appl. Phys. Lett. **94**, 163305 (2009).
[20]W. Holzer, A. Penzkofer, and T. Tsuboi, Chem. Phys. **308**, 93 (2005).
[21]J. Kalinowski, J. Mezyk, F. Meinardi, R. Tubino, M. Cocchi, and D. Virgili, J. Appl. Phys. **98**, 063532 (2005).
[22]S. Athanasopoulos, E. V. Emelianova, A. B. Walker, and D. Beljonne, Phys. Rev. B **80**, 195209 (2009).
[23]S. T. Hoffmann, S. Athanasopoulos, D. Beljonne, H. Bässler, and A. Köhler, J. Phys. Chem. C **116**, 16371 (2012).
[24]O. V. Mikhnenko, J. Lin, Y. Shu, J. E. Anthony, P. W. M. Blom, T.-Q. Nguyen, and M. A. Loi, Phys. Chem. Chem. Phys. **14**, 14196 (2012).
[25]P. K. Watkins, A. B. Walker, and G. L. B. Verschoor, Nano Lett. **5**, 1814 (2005).
[26]C. Groves, R. G. E. Kimber, and A. B. Walker, J. Chem. Phys. **133**, 144110 (2010).
[27]C. Groves and N. C. Greenham, *Multiscale Modelling of Organic and Hybrid Photovoltaics, Topics in Current Chemistry*, edited by D. Beljonne and J. Cornil (Springer, Berlin, 2014), pp. 257–278.
[28]M. Mesta, M. Carvelli, R. J. de Vries, H. van Eersel, J. J. M. van der Holst, M. Schober, M. Furno, B. Lüssem, K. Leo, P. Loebl, R. Coehoorn, and P. A. Bobbert, Nature Mater. **12**, 652 (2013).
[29]E. Engel, K. Leo, and M. Hoffmann, Chem. Phys. **325**, 170 (2006).
[30]B. Valeur, *Molecular Fluorescence: Principles and Applications*, 1st ed. (Wiley-VCH, Weinheim, 2001).
[31]Y. Kawamura, J. Brooks, J. J. Brown, H. Sasabe, and C. Adachi, Phys. Rev. Lett. **96**, 017404 (2006).
[32]G. Scholes, Annu. Rev. Phys. Chem. **54**, 57 (2003).
[33]Y. Divayana and X. W. Sun, Phys. Rev. Lett. **99**, 143003 (2007).
[34]A. Köhler and H. Bässler, Mater. Sci. Eng., R **66**, 71 (2009).